(4)

OFFICE OF NAVAL RESEARCH

Contract N00014-80-K-0852

R&T Code_____

Technical Report No. 44

Utilization of a Hubbard U Model to Understand the Valence Band Photoelectron Data for the High-Temperature Superconductors

By

D. E. Ramaker

Prepared for Publication

in the

Physical Review B

George Washington University
Department of Chemistry
Washington, D.C. 20052

December, 1988

SECURITY CLASSIFICATION OF THIS PAGE

REPORT DOCUMENTATION PAGE

1a. REPORT SECURITY CLASSIFICATION Unclassified	1b. RESTRICTIVE MARKINGS
2a. SECURITY CLASSIFICATION AUTHORITY	3. DISTRIBUTION / AVAILABILITY OF REPORT Approved for Public Release, distribution Unlimited.
2b. DECLASSIFICATION / DOWNGRADING SCHEDULE	
4. PERFORMING ORGANIZATION REPORT NUMBER(S) Technical Report # 44	5. MONITORING ORGANIZATION REPORT NUMBER(S)
6a. NAME OF PERFORMING ORGANIZATION Dept. of Chemistry George Washington Univ.	6b. OFFICE SYMBOL (If applicable)
7a. NAME OF MONITORING ORGANIZATION Office of Naval Research (Code 413)	
6c. ADDRESS (City, State, and ZIP Code) Washington, D.C. 20052	7b. ADDRESS (City, State, and ZIP Code) Chemistry Program 800 N. Quincy Street Arlington, VA 22217
8a. NAME OF FUNDING / SPONSORING ORGANIZATION Office of Naval Research	8b. OFFICE SYMBOL (If applicable)
9. PROCUREMENT INSTRUMENT IDENTIFICATION NUMBER Contract N00014-80-K-0852	
8c. ADDRESS (City, State, and ZIP Code) Chemistry Program 800 North QUINCY, Arlington, VA 22217	10. SOURCE OF FUNDING NUMBERS

PROGRAM ELEMENT NO.	PROJECT NO.	TASK NO. PP	WORK UNIT ACCESSION NO
61153 N		013-08-01	NR 056-681

11. TITLE (Include Security Classification)
Utilization of a Hubbard U Model to Understand the Valence Band Photoelectron Data For the High Temperature Superconductors. (Uncl.)

12. PERSONAL AUTHOR(S)
D. E. Ramaker

13a. TYPE OF REPORT	13b. TIME COVERED	14. DATE OF REPORT (Year, Month, Day)	15. PAGE COUNT
Interim Technical	FROM _____ TO _____	December 1988	11

16. SUPPLEMENTARY NOTATION
Prepared for publication in Physical Review B

17 COSATI CODES		
FIELD	GROUP	SUB-GROUP

18. SUBJECT TERMS (Continue on reverse if necessary and identify by block number)
Superconductivity; Photoelectron Spectroscopy; Hubbard Model; Electron Correlation.

19. ABSTRACT (Continue on reverse if necessary and identify by block number)

The valence band photoelectron spectra are interpreted within a Hubbard model. The 9.5 eV "mystery" peak in the photoelectron spectra for $YBa_2Cu_3O_7$ is identified as arising from a state with two holes localized on nearest neighbor oxygen atoms. Hubbard U parameters are obtained from the data and found to be larger than expected for metallic systems. Keywords: —

20. DISTRIBUTION / AVAILABILITY OF ABSTRACT	21. ABSTRACT SECURITY CLASSIFICATION
☒ UNCLASSIFIED/UNLIMITED ☒ SAME AS RPT. ☐ DTIC USERS	Unclassified
22a NAME OF RESPONSIBLE INDIVIDUAL Dr. David L. Nelson	22b. TELEPHONE (Include Area Code) (202) 696-4410
	22c. OFFICE SYMBOL

DD FORM 1473, 84 MAR — 83 APR edition may be used until exhausted. All other editions are obsolete.

SECURITY CLASSIFICATION OF THIS PAGE
Unclassified

88 12 13 068

We interpret the valence band (VB) photoelectron spectra (UPS and XPS) for the high-temperature superconductors (HTSC's), $La_{2-x}Ba_xCuO_4$ and $YBa_2Cu_3O_7$ (herein referred to as La and 123). We identify the source of the "mystery" feature at 9.5 eV in the UPS [1], and explain the large differences seen between the calculated density of states (DOS) and the experimental spectra in the VB region [2].

The basic VB electronic structure of the HTSC's can be described by an extended Hubbard model, characterized by the transfer or hopping integral t, the Cu and O orbital energies ϵ_d and ϵ_p, the intra-site Coulomb repulsion energies U_d and U_p, and the inter-site repulsion energies U_{dp} and U_{pp}° (i.e. between neighboring Cu-O and O-O atoms). The magnitudes of these U parameters are critical to the mechanism for the superconductivity. As a consequence, much effort has gone into theoretically calculating these parameters, but wide disagreement still exists over the magnitudes. Theoretical values for U_d in the range 6.5-10 eV, U_p (actually U_p-U_{pp}°) in the range 7-14 eV, and U_{dp} in the range 0.6-1.6 eV have been reported [3], with the smaller results favored based on the quality of the calculations. No results for U_{pp}° have been reported. Our empirical results indicate that U_d = 9.5, U_p = 12, and U_{pp}° = 4.5 eV for 123. The latter two are much larger than previously thought for these metallic systems, although U_p-U_{pp}° is in agreement with the best theoretical results above.

We generalize the theory of vanderLaan et al [4] in an extended Hubbard model to interpret the spectra. All of the data can be understood within a $CuO_8^{(2n-2)-}$ cluster model, which is valid when the U's are large relative to the bandwidths [4], i.e. when correlation effects dominate covalent or hybridization effects. Both La and CuO contain CuO_6 groups [5], having 4 short and 2 long Cu-O bonds. The 123 HTSC contains CuO_5 and planar CuO_4

groups [5]. The different n may alter the relative intensities of various features as pointed out below, but similar features are present in each case. The different bond lengths may increase the widths of the spectral features, but little else since correlation dominates.

The $CuO_n^{(2n-g)-}$ cluster has one hole shared between the Cu 3d and O 2p shells in the ground state, which we term the v (valence) states. We indicate the location of the v hole by d (Cu 3d) or p (O 2p). In the case of two holes on the oxygens, we distinguish two holes on the same O (p^2), on ortho neighboring O atoms (pp^o), or on para O atoms (pp^p) of the cluster. Furthermore, neighboring pp^o holes can dimerize [6], so we distinguish between two holes in bonded (pp^o_b) and antibonded (pp^o_a) O pairs.

Most of the O atoms actually participate in two CuO_n clusters. Consistent with previous work [7], we account for this by defining the effective parameter, $\epsilon_p = \epsilon_p' + U_{pe}$, where U_{pe} includes the interaction of a hole in an O p orbital with its environment. In general U_{pe} wil be less than U_{dp} due to polarization.

The v states, as reflected by the theoretical DOS [2], can be described as having the Cu-O bonding ($\dagger_b$) and antibonding ($\dagger_a$) orbitals centered at 4 and 0 eV and the nonbonding Cu and O orbitals at 2 eV. The O features each have a width 2Γ = 4 eV due to the O-O bonding and antibonding character and the Cu-O dispersion. The $\dagger_b$ and $\dagger_a$ wavefunctions can be expressed as [4],

$$\dagger_a = d\cos\vartheta_1 - p\sin\vartheta_1 \qquad (1a)$$

$$\dagger_b = d\sin\vartheta_1 + p\cos\vartheta_1, \qquad (1b)$$

where $\vartheta_1 = 0.5\tan^{-1}(2t/\Delta)$. We also define the Cu-O hybridization shift $\delta_1 = 0.5\,\mathrm{sqrt}(\Delta^2+4t^2) - \Delta/2$, which is utilized in Table 1 to give the energies. In this picture, the ground state of an average CuO_n cluster is located at 1 eV

having the energy $\epsilon_d - \delta_1 + \Gamma/2 = \epsilon_d - \alpha$, which we use as a reference energy for the v^2 states. In CuO, the hybridization shift Γ is smaller, and we shall see below that $\Delta = \epsilon_p - \epsilon_d$ has increased to 1 eV. This increase can be attributed to an increase in ϵ_p, or U_{pd}, and reflects a smaller lattice polarization response due to the more ionic character in CuO.

The photoemission process involves excitation from the ground v state (i.e. the ψ_a state) to the v^2 states. Consistent with the final state rule [8], the photoelectron spectra reflect the v^2 DOS, not the v DOS. In a highly correlated system, the v and v^2 DOS are very different, explaining the well-known differences seen [2] between the theoretical DOS and the photoelectron spectra for the HTSC's.

Table 1 lists the 6 different v^2 configurations. These configurations hybridize, i.e. 1,2,5 & 6 have the same symmetry and mix together to give $\psi_a = \Sigma_a c_{as}\varphi_s$. The coefficients c_{as} are obtained by diagonalizing the 4x4 Hamiltonian matrix, assuming each of the 4 configurations (pp^p, dp, d^2, & p^2) are orthogonal, and that pp^p, p^2, and d^2 have non-zero off-diagonal matrix elements with dp but zero with each other. The two pp^o states (3 & 4) have different symmetry and mix separately. The sudden approximation and the cross-sections for ionization from the O 2p and Cu 3d shells, σ_p and σ_d, can then be utilized to give the expected relative photoemission intensities,

$$I(m) = \Sigma_i \, (\langle \psi_a \psi_i | \psi_m \rangle)^2 \quad \sigma_i = \Sigma_i \, (\Sigma_s \, c_{as} \, \langle \psi_a \psi_i | \varphi_s \rangle)^2 \quad \sigma_i, \qquad (2)$$

for the six v^2 states. In eq. 2, ψ_i indicates the orbital of the hole created by the photoemission process, either d or p, where the new p hole may be created ortho, para or on the same O atom as the initial p hole, (i.e. to create the pp^o, p^2, or pp^p configurations with relative cross-section $\sigma_i = \sigma_p/n$, $(n-2)\sigma_p/n$, and σ_p/n, respectively). σ_p/σ_d is roughly 2. for 21 eV, 1. for 45, and 0.3 for 100 eV photons [2,9]. Results from eq. 2 utilizing the parameters

in Table 1 are given in Fig. 2. States 1 & 2 and 3 & 4 are heavily mixed so that they are the only ones to experience a significant hybridization shift, δ_2 and Γ, as shown in Table 1.

At low photon energies, the sudden approximation assumed above breaks down [10]. The opposite extreme, the adiabatic limit, gives intensity only in the lowest state of each symmetry, 1 and 3, since the system is able to relax before escape of the photoelectron. Since the relaxation time goes as the reciprocal of the shakeup energy [10], we expect that the high energy features, such as the d^2 and p^2 "satellites", will have much smaller intensity than that predicted by eq. 2.

The valence band features. Photon energy dependent data [11-13] in Figure 1 show that the VB features around 5.5 eV in CuO and 2.5 and 5 eV in 123 arise more from σ_p, and the feature at 3 in CuO and 4.2 eV in 123 from σ_d [13-15]. Based on our estimated energies, for CuO we assign the 5.5-eV feature to pp^e_a and pp^p and the 3-eV to dp. In 123, we assign the 5-eV to pp^e_a, the 4.2 to dp, and the 2.5 to pp^p, where we indicate the dominant character of each hybridized state.

These assignments are also consistent with the results in Fig. 2. At low $h\nu$ when σ_p dominates σ_d, $I(pp^e) + I(2)$ is about equal to I(1) at $\Delta = 1$ in agreement with the data for CuO, while it is much greater than I(1) at $\Delta = 0$ in agreement with the data for 123. At large $h\nu$ when σ_d dominates σ_p, I(1) and I(2) dominate. The calculated results in Fig. 2 indicate that I(1)/I(2) should equal about 1 at $\Delta = 1$, and about 0.5 at $\Delta = 0$, whereas the XPS results in Fig. 1 indicate that these ratios are qualitatively much larger. The enhancement of I(1) in both cases arises because of intensity transfer from the d^2 state as a result of relaxation, which occurs even at XPS energies.

A character switch of state 1 from more dp to pp^p and vice versa for

state 2 between CuO and 123 arises because Δ decreases from 1 eV to 0 eV. The smaller Δ in 123, due to a smaller ϵ_p or U_{pp}, is consistent with the Cu 2p XPS and XES data to be discussed elsewhere [16]. States 1 and 2 remain a few eV apart in spite of this switch because of the heavy CI mixing. Since state 1 is more of pp^0 character in the SC's, the additional "charge carrier holes" (present in the La after Sr doping and in the 123 when 7-x is greater than 6.5) are more on the oxygens.

Angle resolved PES data on single crystals of 123 show that the 2.5 eV feature is the only one which shows a small angular dispersion and a photon energy dependence [13]. The near lack of dispersion is consistent with our highly correlated cluster model. The small dispersion of the 2.5 eV feature probably comes from inter-CuO_4 cluster interaction, which is expected to be the largest when both holes are on the bordering O atoms.

The d^2 satellite. The principal multiplet of the d^2 final state for CuO is known to fall at 12.5 with a smaller one around 10 eV [11]. The intensity of the d^2 final state is enhanced by the Cu 2p → 3d (or 2p → 4sp in Cu_2O and Cu) resonant excitation process followed by an Auger decay [11]. This process is resonant between 72-80 eV. The SC's exhibit a behavior similar to CuO [14]. The satellites in Cu_2O and Cu do not have non-resonant components [11] because the UPS for Cu_2O and Cu reflect the one-hole DOS. However, the VB XPS of CuO and the HTSC's can and do show a significant nonresonant d^2 satellite (see Figure 1) [17]; indeed, it should grow as one approaches the sudden limit. This possibility makes it even more difficult to interpret the data for the HTSC's, since the d^2 satellite at 12.5 in the VB XPS falls at or near the same energy as the Ba spin-orbit split 5p features [1], which have been very controversial.

For the XPS (Figure 1a), Miller et al [1] have indicated that the 12.5 eV

feature results from the Ba representative of the bulk, and the 14 and 16 eV features result from Ba bonded to OH^- and $CO_3^=$ on the surface. Steiner et al [18] indicate that the 12.5 eV feature is representative of those Ba atoms surrounded by O atoms, but that the 14 and 16 eV features arise from those Ba atoms with either neighboring O defects or O atoms with holes (i.e. O^- instead of O_2^-). Recent data [13] on single crystals cleaved in-situ (Fig. 1), when impurities are not expected, reveal only the 14 and 16 eV features at glancing emission (i.e. representative of the surface), and two additional features shifted up by about 1 eV at normal emission (i.e. more representative of the bulk). This shift has been interpreted as a surface chemical shift, but it is actually consistent with the Steiner data and interpretation, if one assumes more O defects exist at the surface than in the bulk. Recently Weaver et al [19] reported XPS data for sintered 123 which actually revealed only the features at 12.5 and 14 eV. This indicates either that their surfaces were free of impurities or that the bulk and surface were totally oxidized (i.e. within the Miller or Steiner interpretations). More experimental data is required here to conclusively decide on these two alternatives, but in our opinion the Steiner interpretation appears the more plausible at this time. Regardless of the interpretation, the intensity of the d^2 feature is clearly much smaller than that predicted in Fig. 2 because of the relaxation to state 1. Theory indicates that $I(d^2)$ should be smaller in 123 than in CuO, so the amount of the d^2 satellite actually present in the XPS for the HTSC's is still uncertain.

The $pp^6\underline{L}$ feature. The $pp^6\underline{L}$ state is believed to be responsible for the "mystery" peak found at 9.5 eV in the UPS. Although initially it was thought to arise from carbon on the surface [20], more recent data [13, 21] (Fig. 1b) indicate that it is intrinsic to the material. Figure 1b indicates that such a

feature also appears for CuO [11,12]. This feature does not appear for Cu_2O, as expected since UPS reflects the one-hole DOS in Cu_2O. Thus this feature is not unique to the SC's; it naturally appears for those systems with two-hole photoemission final states.

The 9.5 eV feature has a cross-sectional dependence similar to σ_p [14,15], consistent with the pp^o identification. Figure 2 gives the combined intensity, $I(pp^o_b) + I(pp^o_a)$. We expect that $I(pp^o_b)/I(pp^o_a)$ will be near 1 at XPS energies (this may also depend on the n in CuO_n), and will be much smaller at UPS energies due to relaxation. Therefore $I(pp^o_b)$ should decrease because of relaxation, but increase because of σ_p as $h\nu$ decreases. A small contribution also exists from σ_d so that it is visible even at XPS energies. The data show that $I(pp^o_b)$ is larger for 123 than for CuO and La. This is consistent with Fig. 2, and with the larger pp^o cross-section expected for smaller n.

An upper estimate of the two-center pp^o hole-hole repulsion, U_{pp^o}, can be obtained from the Klopman approximation [22],

$$U_{ij} = e^2/(r_{ij}^2 + (2e^2/(U_i + U_j))^2)^{1/2}, \qquad (3)$$

where r_{ij} is the interatomic distance and U_i and U_j are the corresponding intra-atomic repulsion energies. Equation 2 gives a value for U_{pp^o} around 4.8 eV assuming r_{o-o} is 2.7 A°. The experimental energies of 9.5 and 5.0 eV for pp^o_b and pp^o_a in 123 suggests that the pp^o final state energy is 7.2 eV. This gives an empirical estimate for U_{pp^o} of 4.2 eV, very close to the Klopman theoretical result, which does not include the effects of interatomic screening.

The above result shows that metallic screening of two holes, which are spatially separated on neighboring O atoms, is not very significant. This is in contrast to two Cu-O holes, where Table 1 indicates the optimal $U_{dp} = 1$ eV, while eq. 2 estimates U_{dp} at 6.1 eV assuming r_{Cu-o} is 1.9 A°. This large

reduction in U_{dp} may result from charge transfer into the Cu 4sp levels to screen the Cu–O holes. Although metallic screening, which results from virtual electron-hole (e–p) pair excitations at the Fermi level, is not expected to be large in an insulator such as CuO, screening effects are expected to be much larger in metals, such as the HTSC's. The above results show that U_{dp} is significantly reduced in both, and U_{pp}^{o} remains large in both. The lack of a significant change in the U's between CuO and the HTSC's indicates that the DOS at the Fermi level in the HTSC's must be very small.

The assignment of the 9.5 eV feature explains some of its interesting characteristics. Comparison of data [14] for $YBa_2Cu_3O_x$ (123_x) with O levels at x = 6.95, 6.5, and 6.05 reveal that the reduced O materials, $123_{6.5}$ and $123_{6.05}$, have two peaks around 9.4 and 11.5 eV. It is known that the oxygen decrease resulting from quenching or heating in vacuum occurs primarily from the CuO_4 chains [23]. This may leave distorted CuO_4 or even peroxide O_2^{-} clusters [6] which have an O–O distance less than that in the ordered CuO_4 groups, and hence a larger U_{pp}^{o}. A U_{pp}^{o} of 6.5 eV requires an O–O distance of less than 2 A°. Very recent data [24] on the new Bi and Th type HTSC's indicate a single feature around 10 eV similar to that for 123.

The p^4 feature. Evidence for the existence of the p^4 feature, estimated to appear at 17.5 eV for CuO can indeed be found around 17 eV in the XPS for CuO in Figure 1. UPS data for 123 [13] may reveal the p^4 feature around 16 eV, moved up by at least 1 eV as predicted. Figure 1 shows UPS at hν = 100 and 40 eV. The relative intensity of these two peaks changes when normally one would expect the relative intensity of the $5p_{1/2}$ and $5p_{3/2}$ peaks to remain constant with photon energy. But, the 40 eV spectrum should have a larger σ_p contribution. This suggests that the hν = 40 eV spectrum may have a contribution from the p^4 state, such as that indicated in Figure 1.

Its intensity may arise as much from σ_d as from σ_s at large $h\nu$, although we indicate only the σ_p component in Fig. 2. Its theoretical intensity is remarkably independent of Δ. At low $h\nu$, when σ_p dominates, its intensity remains small because of relaxation.

In summary, we have obtained a set of Hubbard parameters and derived intensity expressions which consistently predict the various features seen in the UPS data. The U's involving the O atoms, U_p and $U_{pp'}$, are much larger in the metallic HTSC's than expected. We have assigned the UPS feature at 9.5 eV, and explained its characteristics. We will show elsewhere [16] that the Hubbard parameters determined here are consistent with core level XPS, x-ray emission and absorption, and Auger data.

TABLE 1 Summary of hole states revealed in the photoelectron data, and estimated energies using the following optimal values for the Hubbard parameters in eV[a]:

$\delta_1 = 2$	$\varepsilon_d = 2$	$U_p = 12, 13$	$U_d = 9.5, 10.2$
$\delta_2 = 0.5, 0.8$	$\varepsilon_p = 2, 3$	$U_{pp}^{\bullet} = 4.5, 4$	$U_{dp} = 1$
$\Gamma = 2$	$U_{pp}^{p} = 0.$	$\alpha = 1, 0.5$	$\Delta = 0, 1.$

State[b]	Energy expression	Calc. E. eV[c,d]	Exp. E. eV[c]	Remark
G.S. and IPES, v^0				
ψ_a) d	$\varepsilon_d - \delta_1 \mp \Gamma$	0 ∓ 2	-	heavily mixed
ψ_b) p	$\varepsilon_p + \delta_1 \mp \Gamma$	4 ∓ 2	-	heavily mixed
UPS and XES, v^2				
1)[e] pp^p	$\varepsilon_p + \Delta - \delta_2 + \alpha$	2.5	2.5	heavily mixed
2)[e] dp	$\varepsilon_p + U_{dp} + \delta_2 + \alpha$	4.5	4.2	heavily mixed
3) $pp^{\bullet}{}_a$	$\varepsilon_p + \Delta + U_{pp}^{\bullet} - \Gamma + \alpha$	5.5	5.	
4) $pp^{\bullet}{}_b$	$\varepsilon_p + \Delta + U_{pp}^{\bullet} + \Gamma + \alpha$	9.5	9.5	mystery peak
5) d^2	$\varepsilon_d + U_d + \alpha$	12.5	12.5	Cu sat.
6) p^2	$\varepsilon_p + \Delta + U_p + \alpha$	15	16	

[a]Parameters for 123 indicated first, those for CuO second.
[b]The dominant character in the hybridized states is given.
[c]The Calc. E and Exp. E columns indicate the results for 123.
[d]The calculated E is defined relative to the ground v^1 (d) state energy = $\varepsilon_d - \alpha$. The v^1(d) energy defines the Fermi level relative to the vacuum level at zero.
[e]The dominant character switches as described in the text, and thus the sign in front of δ_2 is the opposite for CuO.

References

‡Supported in part by the Office of Naval Research

1. D.C. Miller et al., in Thin Film Processing and Characterization of High Temperature Superconductors, J.M. Harper, J.H. Colton, and L.C. Feldman, Eds., AVS Series No. 3 (AIP: New York, 1988) p 336.
2. J. Redinger et al., Phys. Lett. 124, 463 (1987); 469 (1987).
3. C.F. Chen et al., unpublished; A.K. McMahan, R.M. Martin, and S. Satpathy, unpublished; M. Schluter, M.S. Hybertsen, and N. E. Christensen, Proc. Intn. Conf. High T_c Superconductors and Materials and Mechanisms of Superconductivity, J. Muller and J.L. Olsen, Eds., (Interlaken, Switzerland, 1988).
4. G. vanderLaan et al., Phys. Rev. 24, 4369 (1981); J.C. Fuggle et al., Phys. Rev. B37, 1123 (1988).
5. J.E. Greedan et al., Phys. Rev. B35, 8770 (1987).
6. R.A. de Groot et al, Sol. State Commun. 63, 451 (1987); W. Folkerts et al., J. Phys. C: Solid State Phys. 20, 4135 (1987); A. Manthiram et al., Phys. Rev. B37, 3734 (1988).
7. J.E. Hirsch et al., Phys. Rev. Letters 60, 1168 (1988).
8. D.E. Ramaker, Phys. Rev. B25, 7341, (1982).
9. M. Tang et al., Phys. Rev. B, accepted for publ.
10. J. W. Gadzuk and M. Sunjic, Phys. Rev. B12, 524 (1975).
11. M.R. Thuler, R.L. Benbow, and Z. Hurych, Phys. Rev. B26, 669 (1982).
12. C. Benndorf et al., J. Electron. Spectrosc. Related Phenom. 19, 77 (1980).
13. N.G. Stoffel et al., Phys. Rev. B37, 7952 (1988); B38, July (1988).
14. R. Kurtz et al., Phys. Rev. B35, 8818 (1987); D. Mueller et al., in Novel Mechanisms of Superconductors, S.A. Wolf and V.Z. Fresin, Eds.,(Plenum: New York, 1987), p 829.

15. M. Tang et al., Phys. Rev. B37, 1611 (1988).

16. D.E. Ramaker, N.H. Turner, and F.L. Hutson, submitted.

17. A. Rosencwaig and G.K. Wertheim, J. Elect. Spectrosc. Related Phenom. 1, 493 (1972/73).

18. P. Steiner et al., Z. Phys. B - Condensed Matter 69, 449 (1988); Appl. Phys. A44, 75 (1987).

19. J. Weaver et al, preprint.

20. B. Reihl et al., Phys. Rev. B35, 8804 (1987).

21. A. Samsavar et al., Phys. Rev. B37, 5164 (1988).

22. G. Klopman, J. Am. Chem. Soc. 86, 4550 (1964).

23. J.H. Brewer et al., Phys. Rev. Lett. 60, 1073 (1988).

24. Y. Chang et al., preprint; M. Onellion et al., preprint.

Figure Captions

Figure 1a) Comparison of photoelectron spectra in the range 10-18 eV for 123. Data from refs. 13 ($h\nu$ = 100 and 40) and 1 ($h\nu$ = 1487).

1b) Comparison of UPS spectra for CuO and 123 taken with the indicated photon energies in eV. Data for CuO from refs. 17 ($h\nu$ = 1487), 11 ($h\nu$ = 74) and 12 ($h\nu$ = 21). Data for 123 from ref. 13 ($h\nu$ = 25 and 74) and 1 ($h\nu$ = 1487).

Figure 2) Calculated photoemission intensities for the v^1 states obtained from evaluation of eq. 2, utilizing the parameters in Table 1 for CuO_4 clusters. The intensities have been normalized so that the sum is $\sigma_p + \sigma_d$.

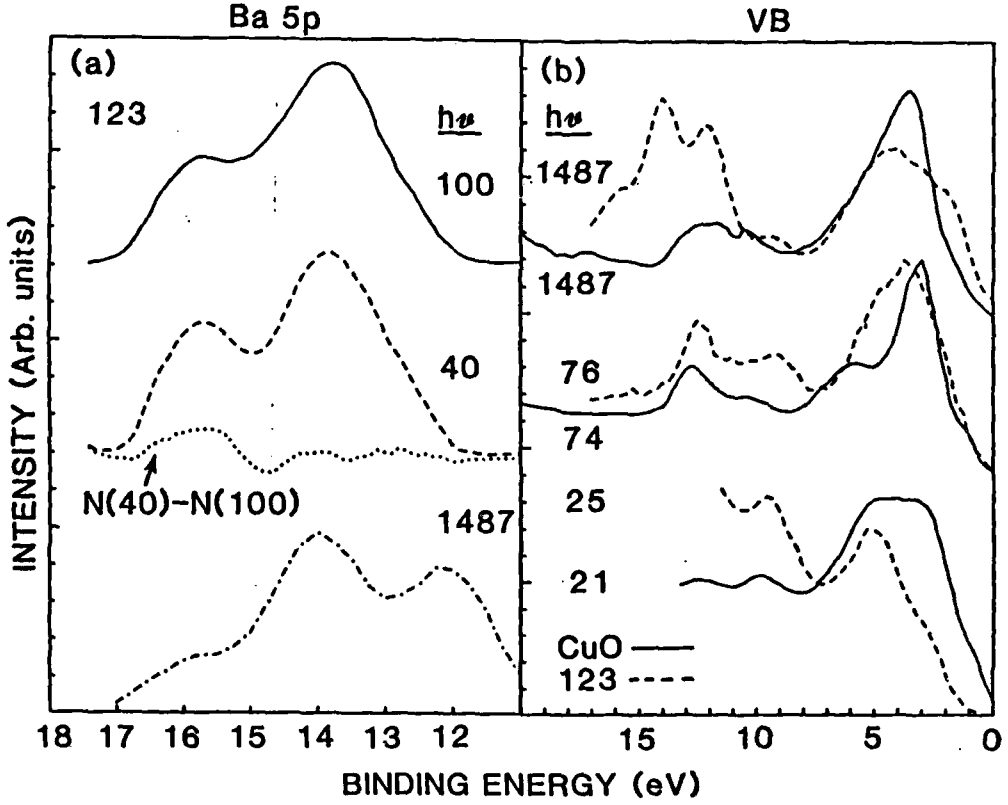
Ba 5p
VB
(a)
(b)
123
hν
100
40
N(40)-N(100)
1487
1487
1487
76
74
25
21
CuO
123
INTENSITY (Arb. units)
18 17 16 15 14 13 12
15 10 5 0
BINDING ENERGY (eV)

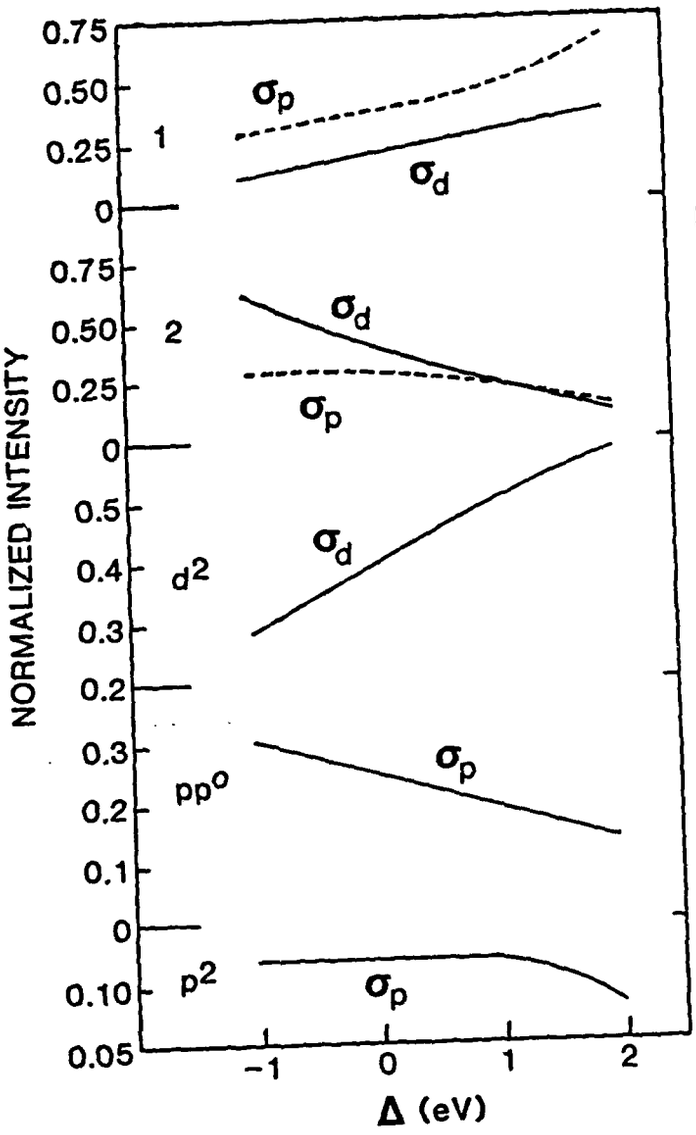
NORMALIZED INTENSITY
0.75
0.50
0.25
0
1
σ_p
σ_d
0.75
0.50
0.25
0
2
σ_d
σ_p
0.5
0.4
0.3
0.2
d^2
σ_d
0.3
0.2
0.1
0
pp^o
σ_p
0.10
0.05
p^2
σ_p
−1
0
1
2
Δ (eV)

TECHNICAL REPORT DISTRIBUTION LIST, GEN

	No. Copies
Office of Naval Research Attn: Code 1113 800 N. Quincy Street Arlington, Virginia 22217-5000	2
Dr. Bernard Douda Naval Weapons Support Center Code 50C Crane, Indiana 47522-5050	1
Naval Civil Engineering Laboratory Attn: Dr. R. W. Drisko, Code L52 Port Hueneme, California 93401	1
Defense Technical Information Center Building 5, Cameron Station Alexandria, Virginia 22314	12 high quality
DTNSRDC Attn: Dr. H. Singerman Applied Chemistry Division Annapolis, Maryland 21401	1
Dr. William Tolles Superintendent Chemistry Division, Code 6100 Naval Research Laboratory Washington, D.C. 20375-5000	1
Dr. David Young Code 334 NORDA NSTL, Mississippi 39529	1
Naval Weapons Center Attn: Dr. Ron Atkins Chemistry Division China Lake, California 93555	1
Scientific Advisor Commandant of the Marine Corps Code RD-1 Washington, D.C. 20380	1
U.S. Army Research Office Attn: CRD-AA-IP P.O. Box 12211 Research Triangle Park, NC 27709	1
Mr. John Boyle Materials Branch Naval Ship Engineering Center Philadelphia, Pennsylvania 19112	1
Naval Ocean Systems Center Attn: Dr. S. Yamamoto Marine Sciences Division San Diego, California 91232	1

ABSTRACTS DISTRIBUTION LIST, 056/625/629

Dr. F. Carter
Code 6170
Naval Research Laboratory
Washington, D.C. 20375-5000

Dr. Richard Colton
Code 6170
Naval Research Laboratory
Washington, D.C. 20375-5000

Dr. Dan Pierce
National Bureau of Standards
Optical Physics Division
Washington, D.C. 20234

Dr. R. G. Wallis
Department of Physics
University of California
Irvine, California 92664

Dr. D. Ramaker
Chemistry Department
George Washington University
Washington, D.C. 20052

Dr. J. C. Hemminger
Chemistry Department
University of California
Irvine, California 92717

Dr. T. F. George
Chemistry Department
University of Rochester
Rochester, New York 14627

Dr. G. Rubloff
IBM
Thomas J. Watson Research Center
P.O. Box 218
Yorktown Heights, New York 10598

Dr. J. Baldeschwieler
Department of Chemistry and
Chemical Engineering
California Institute of Technology
Pasadena, California 91125

Dr. Galen D. Stucky
Chemistry Department
University of California
Santa Barbara, CA 93106

Dr. A. Steckl
Department of Electrical and
Systems Engineering
Rensselaer Polytechnic Institute
Troy, New York 12181

Dr. John T. Yates
Department of Chemistry
University of Pittsburgh
Pittsburgh, Pennsylvania 15260

Dr. R. Stanley Williams
Department of Chemistry
University of California
Los Angeles, California 90024

Dr. R. P. Messmer
Materials Characterization Lab.
General Electric Company
Schenectady, New York 22217

Dr. J. T. Keiser
Department of Chemistry
University of Richmond
Richmond, Virginia 23173

Dr. R. W. Plummer
Department of Physics
University of Pennsylvania
Philadelphia, Pennsylvania 19104

Dr. E. Yeager
Department of Chemistry
Case Western Reserve University
Cleveland, Ohio 41105

Dr. N. Winograd
Department of Chemistry
Pennsylvania State University
University Park, Pennsylvania 16802

Dr. Roald Hoffmann
Department of Chemistry
Cornell University
Ithaca, New York 14853

Dr. Robert L. Whetten
Department of Chemistry
University of California
Los Angeles, CA 90024

Dr. Daniel M. Neumark
Department of Chemistry
University of California
Berkeley, CA 94720

Dr. G. H. Morrison
Department of Chemistry
Cornell University
Ithaca, New York 14853

ABSTRACTS DISTRIBUTION LIST, 056/625/629

Dr. J. E. Jensen
Hughes Research Laboratory
3011 Malibu Canyon Road
Malibu, California 90265

Dr. J. H. Weaver
Department of Chemical Engineering
and Materials Science
University of Minnesota
Minneapolis, Minnesota 55455

Dr. A. Reisman
Microelectronics Center of North Carolina
Research Triangle Park, North Carolina
27709

Dr. M. Grunze
Laboratory for Surface Science
and Technology
University of Maine
Orono, Maine 04469

Dr. J. Butler
Naval Research Laboratory
Code 6115
Washington D.C. 20375-5000

Dr. L. Interante
Chemistry Department
Rensselaer Polytechnic Institute
Troy, New York 12181

Dr. Irvin Heard
Chemistry and Physics Department
Lincoln University
Lincoln University, Pennsylvania 19352

Dr. K. J. Klaubunde
Department of Chemistry
Kansas State University
Manhattan, Kansas 66506

Dr. C. B. Harris
Department of Chemistry
University of California
Berkeley, California 94720

Dr. R. Bruce King
Department of Chemistry
University of Georgia
Athens, Georgia 30602

Dr. R. Reeves
Chemistry Department
Renssaeler Polytechnic Institute
Troy, New York 12181

Dr. Steven M. George
Stanford University
Department of Chemistry
Stanford, CA 94305

Dr. Mark Johnson
Yale University
Department of Chemistry
New Haven, CT 06511-8118

Dr. W. Knauer
Hughes Research Laboratory
3011 Malibu Canyon Road
Malibu, California 90265

Dr. Theodore E. Madey
Surface Chemistry Section
Department of Commerce
National Bureau of Standards
Washington, D.C. 20234

Dr. J. E. Demuth
IBM Corporation
Thomas J. Watson Research Center
P.O. Box 218
Yorktown Heights, New York 10598

Dr. M. G. Lagally
Department of Metallurgical
and Mining Engineering
University of Wisconsin
Madison, Wisconsin 53706

Dr. R. P. Van Duyne
Chemistry Department
Northwestern University
Evanston, Illinois 60637

Dr. J. M. White
Department of Chemistry
University of Texas
Austin, Texas 78712

Dr. Richard J. Saykally
Department of Chemistry
University of California
Berkeley, California 94720

ABSTRACTS DISTRIBUTION LIST, 056/625/629

Dr. G. A. Somorjai
Department of Chemistry
University of California
Berkeley, California 94720

Dr. J. Murday
Naval Research Laboratory
Code 6170
Washington, D.C. 20375-5000

Dr. W. T. Peria
Electrical Engineering Department
University of Minnesota
Minneapolis, Minnesota 55455

Dr. Keith H. Johnson
Department of Metallurgy and
Materials Science
Massachusetts Institute of Technology
Cambridge, Massachusetts 02139

Dr. S. Sibener
Department of Chemistry
James Franck Institute
5640 Ellis Avenue
Chicago, Illinois 60637

Dr. Arold Green
Quantum Surface Dynamics Branch
Code 3817
Naval Weapons Center
China Lake, California 93555

Dr. A. Wold
Department of Chemistry
Brown University
Providence, Rhode Island 02912

Dr. S. L. Bernasek
Department of Chemistry
Princeton University
Princeton, New Jersey 08544

Dr. W. Kohn
Department of Physics
University of California, San Diego
La Jolla, California 92037

Dr. Stephen D. Kevan
Physics Department
University Of Oregan
Eugene, Oregon 97403

Dr. David M. Walba
Department of Chemistry
University of Colorado
Boulder, CO 80309-0215

Dr. L. Kesmodel
Department of Physics
Indiana University
Bloomington, Indiana 47403

Dr. K. C. Janda
University of Pittsburg
Chemistry Building
Pittsburg, PA 15260

Dr. E. A. Irene
Department of Chemistry
University of North Carolina
Chapel Hill, North Carolina 27514

Dr. Adam Heller
Bell Laboratories
Murray Hill, New Jersey 07974

Dr. Martin Fleischmann
Department of Chemistry
University of Southampton
Southampton S09 5NH
UNITED KINGDOM

Dr. H. Tachikawa
Chemistry Department
Jackson State University
Jackson, Mississippi 39217

Dr. John W. Wilkins
Cornell University
Laboratory of Atomic and
Solid State Physics
Ithaca, New York 14853

Dr. Ronald Lee
R301
Naval Surface Weapons Center
White Oak
Silver Spring, Maryland 20910

Dr. Robert Gomer
Department of Chemistry
James Franck Institute
5640 Ellis Avenue
Chicago, Illinois 60637

Dr. Horia Metiu
Chemistry Department
University of California
Santa Barbara, California 93106

Dr. W. Goddard
Department of Chemistry and Chemical
Engineering
California Institute of Technology
Pasadena, California 91125